Earth and Planetary Science Letters 331–332 (2012) 201–209

Contents lists available at SciVerse ScienceDirect

Earth and Planetary Science Letters

journal homepage: www.elsevier.com/locate/epsl

Subglacial Lake Whillans — Seismic observations of a shallow active reservoir beneath a West Antarctic ice stream

Huw J. Horgan [a,*], Sridhar Anandakrishnan [b,c], Robert W. Jacobel [d], Knut Christianson [d], Richard B. Alley [b,c], David S. Heeszel [e], Stefano Picotti [f], Jacob I. Walter [g]

[a] Antarctic Research Centre, Victoria University of Wellington, Kelburn Pde, Wellington, New Zealand
[b] Dept. of Geosciences, Pennsylvania State University, University Park, PA 16802, USA
[c] Earth and Environmental Systems Institute, The Pennsylvania State University, University Park, PA 16802, USA
[d] Department of Physics, St. Olaf College, 1520 St. Olaf Avenue, Northfield, MN 55057, USA
[e] Institute of Geophysics and Planetary Physics, University of California, San Diego, La Jolla, CA 92093, USA
[f] Istituto Nazionale di Oceanografia e di Geofisica Sperimentale (INOGS), Trieste, Italy
[g] Dept. of Earth and Planetary Sciences, University of California, Santa Cruz. CA 95064, USA

ARTICLE INFO

Article history:
Received 19 September 2011
Received in revised form 28 February 2012
Accepted 29 February 2012
Available online 11 April 2012

Editor: P. Shearer

Keywords:
subglacial lakes
glaciology
ice streams
Antarctica
geophysics
seismology

ABSTRACT

Active subglacial lakes concentrate the distribution of water beneath ice sheets in both space and time. Seismic and surface observations from Subglacial Lake Whillans (SLW), West Antarctica, reveal that this active lake forms a persistent, albeit fluctuating, reservoir beneath Whillans Ice Stream. Imaging and phase observations using active-source seismic data show that SLW is a perpetually shallow feature. When surveyed near its low-stand, a water column was resolvable by seismic techniques along only 5 km of the 45 km profiled, with a maximum depth of less than 8 m. Satellite altimetry shows that the high-stand adds no more than 3–4 m to this. This water column presents a suitable drill site at S 84.240° W 153.694°. Elsewhere, the majority of the bed appears wet with soft sediment or water thicknesses of less than the imaging resolution of our data of approximately 2 m. The surface expression of the active lake, previously revealed by ICESat elevation data and image differencing, generally corresponds to the seismic estimate of soft sediment or water, with notable exceptions occurring at the upstream and downstream ends of the lake. These exceptions indicate that SLW's water column is very shallow or absent in places at low-stands, or has disconnected or transiently active and inactive portions.

1. Introduction

It has long been recognized that water at the base of ice sheets plays an important role in ice-sheet dynamics (Engelhardt et al., 1990; Rose, 1979). More recently, remote sensing observations of short-term elevation changes have been used to infer that the hydrologic system beneath the Antarctic Ice Sheet is constantly changing, with exchange between subglacial lakes (Smith et al., 2009; Wingham et al., 2006) and to and from the background subglacial system (Fricker et al., 2007; Gray et al., 2005; Smith et al., 2009). Subglacial lakes have also been credited with initiating the onset of streaming ice (Bell et al., 2007) and shown to be a significant source of subglacial accretion (Bell et al., 2011). All of these recent observations of subglacial lakes are important for studies of ice dynamics as subglacial hydrology in part determines the basal boundary condition beneath glaciers and ice streams, and this boundary partly resists the gravitational driving stress of ice flow. Water under pressure at the bed of a glacier counters the weight of the overriding ice, smooths the effective topography of the bed, and allows the ice and underlying till to flow more easily (Kamb, 2001). Whereas a subglacial drainage network evolves to accommodate a steady water supply (e.g. Röthlisberger, 1972; Walder and Fowler, 1994), fluctuations in water supply are known to lead to velocity changes on glaciers (Iken & Bindschadler, 1986) and ice sheets (Schoof, 2010; Zwally et al., 2002), and subglacial lake drainage has been correlated with the acceleration of at least one major Antarctic outlet glacier (Byrd Glacier; Stearns et al., 2008).

Inventories of Antarctic subglacial lakes, based mainly on radio echo sounding observations (Carter et al., 2007; Siegert et al., 2005), indicate that at least 280 lakes exist beneath the Antarctic Ice Sheet (Smith et al., 2009). Observations of surface elevation change have shown that at least 124 lakes were actively filling and draining beneath the Antarctic ice sheets between 2003 and 2008 (termed active lakes; Smith et al., 2009). At the time of writing, three international programs were preparing to access subglacial lakes in the Antarctic: Lake Vostok (Studinger et al., 2003), Lake Ellsworth (Siegert et al., 2004; Vaughan et al., 2007; Woodward et al., 2010),

* Corresponding author.
E-mail address: huw.horgan@vuw.ac.nz (H.J. Horgan).

0012-821X/$ – see front matter © 2012 Elsevier B.V. All rights reserved.
doi:10.1016/j.epsl.2012.02.023

and SLW (Fricker et al., 2011). Of these, SLW is distinct, as it is a small (59 km^2; Fricker & Scambos, 2009) active lake lying beneath an active ice stream (Whillans Ice Stream) (Fig. 1). Whillans Ice Stream, previously known as Ice Stream B, forms one of the main drainage conduits from the West Antarctic Ice Sheet into the Ross Ice Shelf. Despite its low driving stress, this ice stream flows at over 300 m a^{-1}, achieving this motion in downglacier regions by short, typically diurnal or semi-diurnal, bursts interspersed with long periods of relative quiescence (Bindschadler et al., 2003; Winberry et al., 2009b). In the past decades, the ice stream has been observed to be decelerating, indicating that it may be destined for stagnation (Joughin et al., 2002, 2005). Glaciological drilling and instrumentation in the late 1980s and 1990s showed that water flow beneath Whillans Ice Stream is likely achieved by more-or-less regularly spaced channels or canals in the underlying deformable till (Engelhardt & Kamb, 1997; Kamb, 2001).

Here we report geophysical findings from SLW. We present surface elevation observations from the Ice Cloud and land Elevation Satellite (ICESat) for the entire ICESat observation period of 2003–2009. We combine these observations with newly acquired GPS observations and active source seismic data. The seismic data reveal the presence of water at the bed (Kapitsa et al., 1996; Peters et al., 2007, 2008) and the extent and depth of the subglacial lake. We compare these findings with the active lake extent as determined using remote sensing and surface elevation observations. During the 2010–2011 Antarctic summer, Christianson et al. (2012-this issue) acquired a grid of kinematic GPS and radio echo sounding observations from SLW. We combine our findings with the results of Christianson et al. (2012-this issue) to present a glaciological summary of SLW in preparation for subglacial access.

2. ICESat and GPS surface elevation data

SLW was originally identified by Fricker et al. (2007) using surface elevation observations from the Geoscience Laser Altimeter System (GLAS) aboard ICESat. The 2003–2008 ICESat period was subsequently examined by Fricker and Scambos (2009). The active lakes in the region were also reported by Smith et al. (2009), and both Smith et al. (2005) and Pritchard et al. (2009)) have provided previous estimates of regional surface elevation change. Here we combine data from the entire ICESat period (2003–2009, Data Release 531) with kinematic GPS observations collected during December 2010. We follow the ICESat filtering and processing methodology outlined by Smith et al. (2009) and incorporate GPS data by extracting transects along ICESat orbit tracks from the surface DEM presented by Christianson et al. (2012-this issue).

Data from all ICESat periods and the GPS transects were sorted into 700 m long by 300 m wide bins spaced every 500 m along ICESat reference orbits. Within each bin the ICESat and GPS record times (t), positions, and elevations (z), were fitted by an optimal dipping planar–surface, which was allowed to migrate at a constant $\partial z/\partial t$ (Equation 1, Smith et al., 2009). Optimization minimized the difference between the observed ICESat and GPS elevations and the model planar surface. Residuals to the model surface provided elevation data corrected for cross-track slope and background elevation-change. We present total elevation range $(z_{max} - z_{min})$ (Fig. 2), and

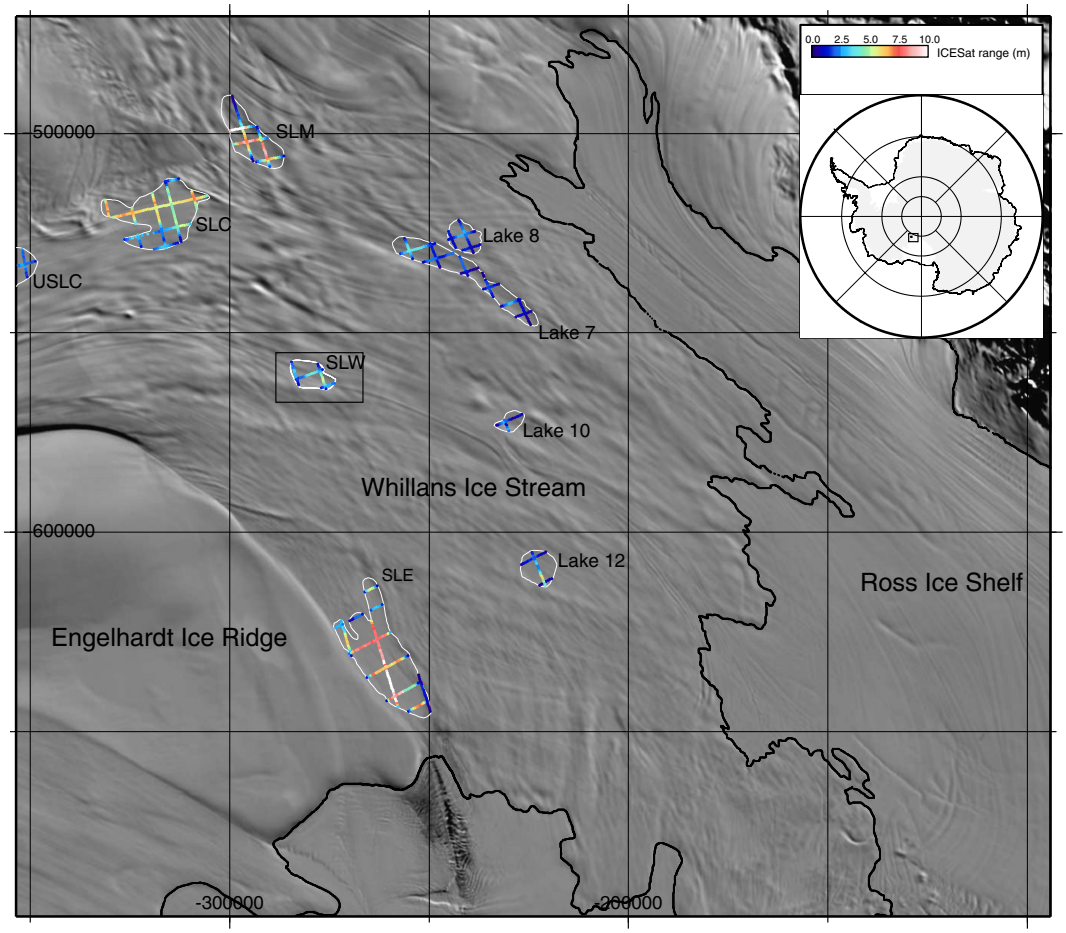

Fig. 1. Whillans Ice Stream with ICESat tracks on the lakes colored by elevation range observed throughout the ICESat period. (See text for discussion). Lake outlines are shown in white and are from Fricker and Scambos (2009). Background imagery and grounding line from MODIS MOA (Haran et al., 2005). Subglacial lake names from Fricker and Scambos (2009): Upper Subglacial Lake Conway (USLC), Subglacial Lake Conway (SLC), Subglacial Lake Mercer (SLM), Subglacial Lake Whillans (SLW), Subglacial Lake Engelhardt (SLE). Polar stereographic projection with true scale at −71°.

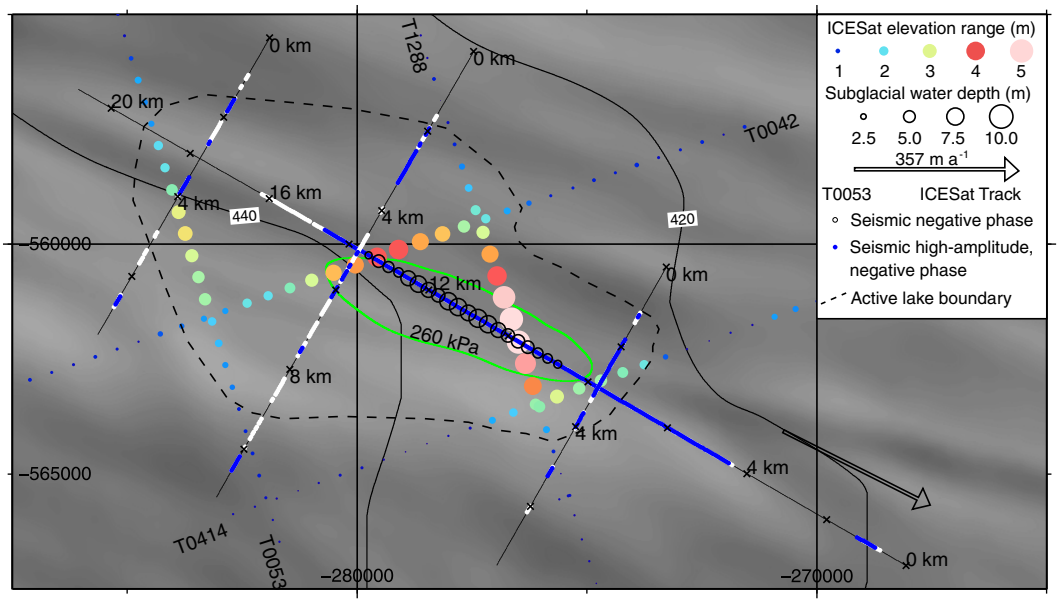

Fig. 2. Location map showing SLW, West Antarctica. Colored circles of variable sizes denote the elevation range of ICESat observations. Empty circles of variable sizes show the thickness of the seismically-imaged water column. The green contour shows the260 kPa hydropotential contour from Christianson et al. (2012-this issue). The blue circles along the seismic profiles denote the high amplitude, negative-polarity bed return. Gray circles show all negative polarity seismic returns. Seismic profile distances are shown in kilometers. Also shown are GPS locations (diamonds) and the outline of the active lake (dashed line, Fricker & Scambos, 2009). Contours show 1997 RADARSAT derived ice velocities in m a^{-1} (Joughin, 2008). Arrow denotes the GPS derived velocity during our campaign. Background imagery from MODIS MOA (Haran et al., 2005). Polar stereographic projection with true scale at −71°.

residual elevations after correction for secular elevation change and cross-track slope ($z - z_{model}$)(Fig. 3).

The Whillans Ice Stream subglacial lakes are highlighted by their elevation ranges of up to ~10 m (Figs. 1–3), the largest elevation ranges being observed on Subglacial Lakes Engelhardt, Mercer, and Conway. SLW exhibits a surface elevation range of up to 5 m and is sampled by four ICESat tracks (Figs. 2–3). Surface elevation at SLW does not change uniformly. Instead the ICESat and GPS residual time series for SLW shows spatial and temporal variability (Fig. 3). Tracks 0042, 0414, and 1288, exhibit high-stands occurring in 2006 (as reported by Fricker & Scambos, 2009). A secondary high-stand period was sampled in 2008 and is the largest high-stand on Tracks 0053 and 0414, while it forms a secondary peak on Track 0042. Tracks 0053 and 0414 appear to be at or near low-stand at the time of our GPS and seismic surveying in December 2010, while, Tracks 0042 and 1288 both are between 1 and 2 m above low-stand at the time of surveying (3–4 m below high-stand). This non-synchronous filling signal is consistent with the hydropotential calculated by Christianson et al. (2012-this issue), as Tracks 0042 and 1288, but not 0053 and 0414, cross the hydropotential low where water would initially collect (Fig. 2). Tracks 0042 and 1288 also exhibit the greatest elevation range of all the SLW ICESat tracks, consistent with their earlier filling signature.

3. Active-source seismology

Four active source seismic profiles were acquired over SLW during the austral summer of 2010–2011 (Fig. 2). One profile was acquired along the long axis of the lake (sub parallel to the ice stream flow direction), and three transverse profiles were acquired across the lake. The main body of the longitudinal profile (kilometers 5–20) was acquired at a nominal fold of 4 (shot spacing of 240 m), whereas the remainder of the longitudinal profile and the transverse profiles were acquired at a nominal fold of 2 (shot spacing of 480 m). Shot and recorder synchronization was accomplished using GPS time signals. Charges, consisting of 0.4 kg of PETN (pentaerythritol tetranitrate), were placed at a nominal depth of 27 m using a hot-water drill. Buried crevasses were often encountered when placing charges. Bridge thicknesses were always in excess of 12 m; however, charges detonated in or proximal to crevasses resulted in incoherent noise likely generated by the spalling of material off of the crevasse walls and bridges. Sensors were spaced every 20 m along the profiles, and consisted of alternating 28 Hz single-string phones and 40 Hz georods. (A georod is a plastic rod approximately 0.5 m long that contains multiple geophone elements.)

Seismic data processing followed land-based techniques with some modifications to suit snow and ice. Crevasse-generated noise was seen across all frequencies and had no distinct spatial-frequency (wavenumber) signature. We removed some crevasse noise by applying a semblance filter after transforming the data to tau-p domain. (Tau-p, or intercept–slowness, domain is another means of representing distance–time domain data). Delays caused by shot propagation in low-velocity crevasses required manual static corrections. Predictive and spiking deconvolution was applied to remove some of the short-path multiple energy and improve the coherence of the seismic record. A stack-power residual static algorithm was applied to account for variability in geophone and shot placement. Finally, the data were migrated at a constant velocity. Our processed seismic data consist of frequencies of ~20–200 Hz, resulting in a maximum vertical resolution of ~5 m in ice and ~2 m in water. Our nominal horizontal-resolution at the base of the ice is ~180 m (Eqn. 4.126, Fowler, 1990). (For seismic profile coordinates see Supplementary Table 1.)

The longitudinal seismic profile (Fig. 4) reveals a flat bed with large regions of reversed polarity indicative of a higher acoustic impedance material (ice) overlying a lower acoustic impedance material (soft-sediment or water). High amplitudes are observed to coincide with many of the reversed polarity bed returns. Our amplitude observations are relative and qualitative as quantitative estimates are complicated by the crevassing noise. However, theoretical Amplitude-Versus-Angle curves show that our observations of high-amplitude, negative-phase returns are consistent with the existence of water at the bed. Fig. 5 shows the P-wave reflection coefficients and corresponding phase angles at the ice bottom. Three cases are considered with ice overlying: water, soft sediments

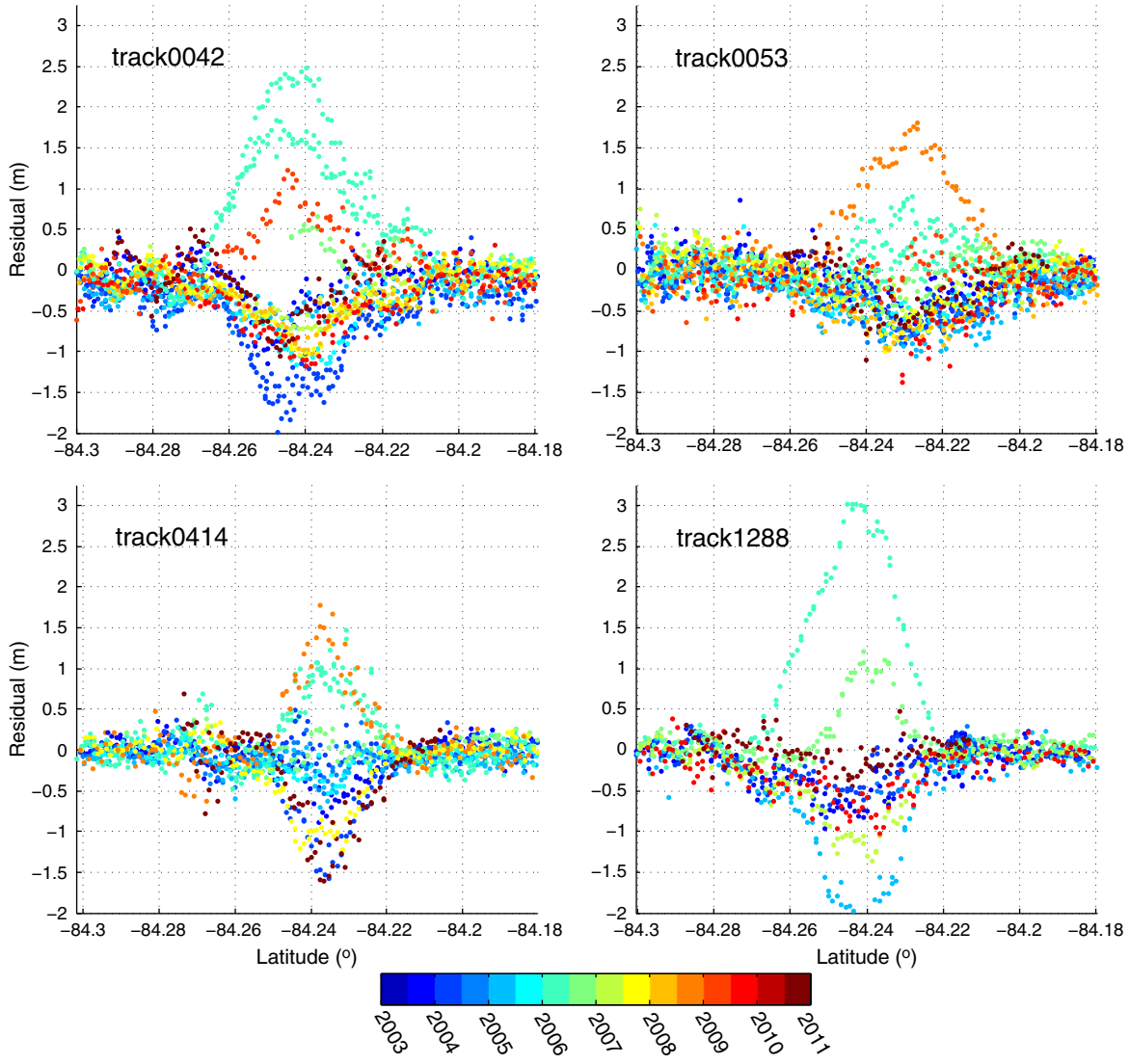

Fig. 3. Residual surface elevation observation over time for the four repeat tracks crossing SLW. (a) Track0042. (b) Track0053. (c) Track0414. (d) Track1288. See Fig. 2 for track locations.

($V_P = 1700\ \mathrm{m\ s^{-1}}$, $V_S = 700\ \mathrm{m\ s^{-1}}$, density $= 2100\ \mathrm{kg\ m^{-3}}$), and normal sediments ($V_P = 2820\ \mathrm{m\ s^{-1}}$, $V_S = 1530\ \mathrm{m\ s^{-1}}$, density $= 2130\ \mathrm{kg\ m^{-3}}$). The reflection coefficients and phase angles are obtained from the Zoeppritz equations generalized to the viscoelastic case, as described in Carcione and Gei (2003). Our data consist of bed incidence-angles of less than 60°. In the longitudinal profile,

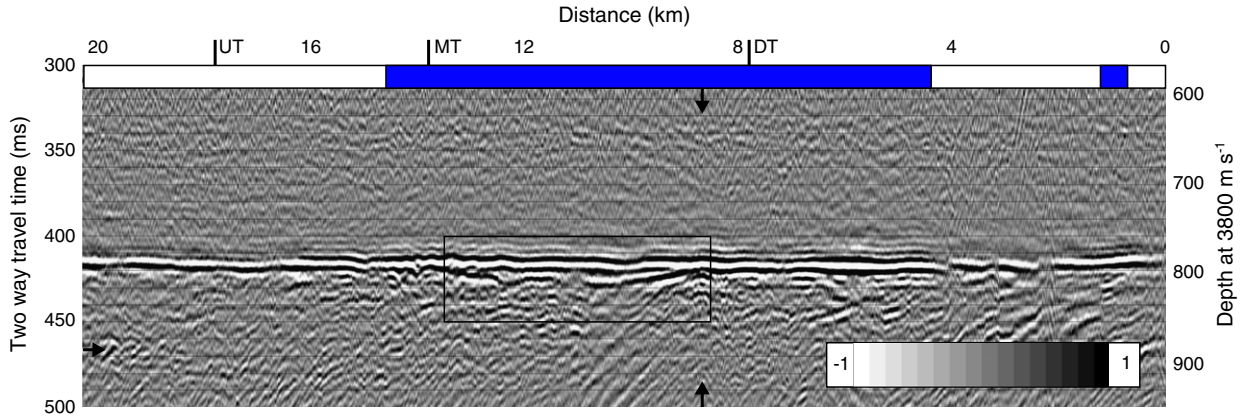

Fig. 4. Longitudinal seismic profile. Ice stream flow is from left to right. See Fig. 2 for location. Inset box shows location of Fig. 7. Seismic polarity convention of this and subsequent profiles follows (Thigpen et al., 1975). Vertical arrows mark the acoustic basement feature mentioned in the text. Similarly, the horizontal arrow marks the acoustic basement. Tick-marks labeled UT, MT, and DT, denote the intersections with the upstream, middle, and downstream transverse profiles respectively (Figs. 8–10). Blue and white bar shows the zones of interpreted water (blue).

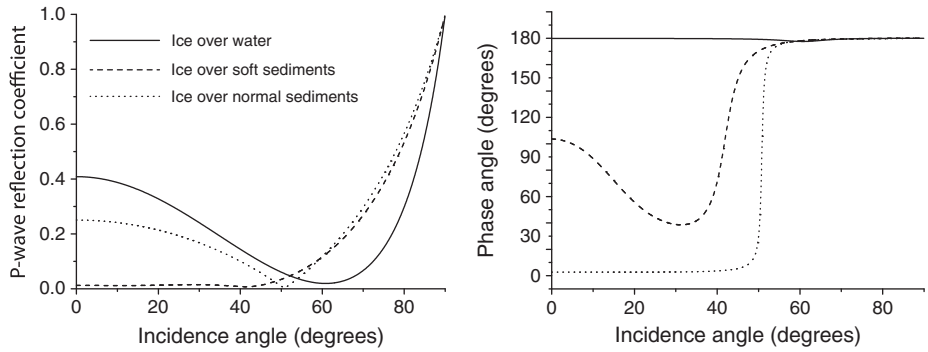

Fig. 5. Theoretical Amplitude-Versus-Angle curves for three possible bed scenarios. Left: P-wave reflection coefficients. Right: phase angles. Case shown are water (solid line), normal sediments (dotted line) and soft sediments (dashed line) overlain by ice. Material properties follow (Anandakrishnan, 2003) and are as follows: (1) Ice, $V_P = 3843\ m\ s^{-1}$, $V_S = 1900\ m\ s^{-1}$, $\rho = 912\ kg\ m^{-3}$, (2) Water: $V_P = 1443\ m\ s^{-1}$, $V_S = 0\ m\ s^{-1}$, $\rho = 1017\ kg\ m^{-3}$, (3) Normalsediments: $V_P = 2817\ m\ s^{-1}$, $V_S = 1530\ m\ s^{-1}$, $\rho = 2128\ kg\ m^{-3}$, (4) Soft sediments: $V_P = 1700\ m\ s^{-1}$, $V_S = 700\ m\ s^{-1}$, $\rho = 2100\ kg\ m^{-3}$. Where V_P denotes compressional-wave velocity, V_S denotes shear-wave velocity, and ρ denotes density.

high amplitude, and reversed polarity returns are observed between kilometers 0.8 and 1.2 and between kilometers 4.5 and 14.6 (Figs. 2, 4). We plot the occurrence of reverse polarity returns, and overlay these with high-amplitude reverse polarity returns, in Fig. 2.

In the central portion of the longitudinal line, at kilometers 8.5–13.5, a prominent positive polarity reflector beneath the ice-bottom interface is observed. This reflector is thought to correspond to the base of the water column and is matched well by synthetic shot-records modeled using a buried 150 Hz Ricker-wave source in a medium of firn and ice overlying a thin water column (Fig. 6). At water compressional-wave velocities, the imaged water column is a maximum of ~8 m thick(Fig. 7). Radio echo sounding cross-profiles (Christianson et al., 2012-this issue) confirm that this feature does not result from any out-of-plane features. The possibility remains that the lower interface is a subglacial sedimentary feature, but we deem this unlikely based on the polarity and amplitude evidence for water at the bed, the character of the sub-bed reflector (it deepens then shallows gradually) and its similarity to the synthetic gathers, and its correspondence with maximum ICESat elevation range. Acoustic basement features form the upstream and downstream ends of the imaged water column (kilometers 13.8 and 8.5 respectively). The downstream basement feature corresponds to a prominent bed-ridge observed in radar profiles throughout the region (Christianson et al., 2012-this issue). At the upstream end of the profile a subtle acoustic basement is apparent at ~460—470 ms. Above this acoustic basement, the subglacial material is seismically opaque indicating massive and homogenous sedimentation. Data quality is poorer downstream of the imaged water-column, but the acoustic basement in this region appears shallower with some internal reflectivity.

The transverse profiles (Figs. 8–10) display similar patterns of reversed polarity and high-amplitudes indicating water at the bed, low-amplitude reverse-phase sections likely due to soft sediments, and positive-polarity and lower amplitude returns indicating more lithified sediments. The upstream transverse profile (Fig. 8) displays high amplitude, reverse polarity returns between kilometers 1.5–1.9, 2.6–2.7, 3.5–3.9, and 6.5–6.7. Similarly the central transverse profile (Fig. 9) displays high amplitude, reverse polarity returns between kilometers 1.9–3.4, 5.1–6.2, 7.4–7.6, and 10.2–10.6. At the downstream end of the lake, the transverse profile (Fig. 10) reveals a narrower lake with high amplitude, reverse polarity returns observed between kilometers 1.2–1.3, 1.8–3.2, 3.6–4.1 and kilometers 5.0–5.2.

4. Discussion

Observations of surface elevation change above SLW are related to seismic observations of water at the bed, but not in a straight-forward manner. We interpret water at the bed based on negative phase, high-amplitude seismic returns. This is consistent with the interpretations of King et al. (2004) and Peters et al. (2007) in their seismic studies of water beneath West Antarctic ice streams. Elsewhere the bed returns are low amplitude and negative phase, which is consistent with the findings of King et al. (2004), or low amplitude and positive

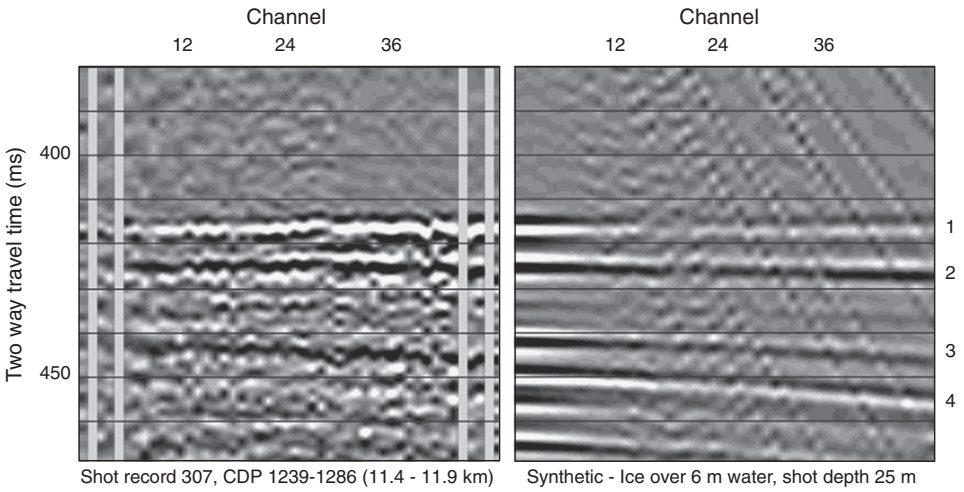

Fig. 6. Left: Shot record 307 with minimal processing. Right: Synthetic shot record calculated using a 150 Hz Ricker-wavelet source buried at 25 m. The medium consists of 40 m of firn ($2000\ m\ s^{-1}$) overlying 732 m of ice ($3750\ m\ s^{-1}$) and 6 m of water ($1430\ m\ s^{-1}$). Annotation on the right hand side denotes: (1) ice bottom, (2) lake bottom, (3) ice bottom shot ghost (peg-leg multiple due to shot burial), (4) lake bottom shot ghost.

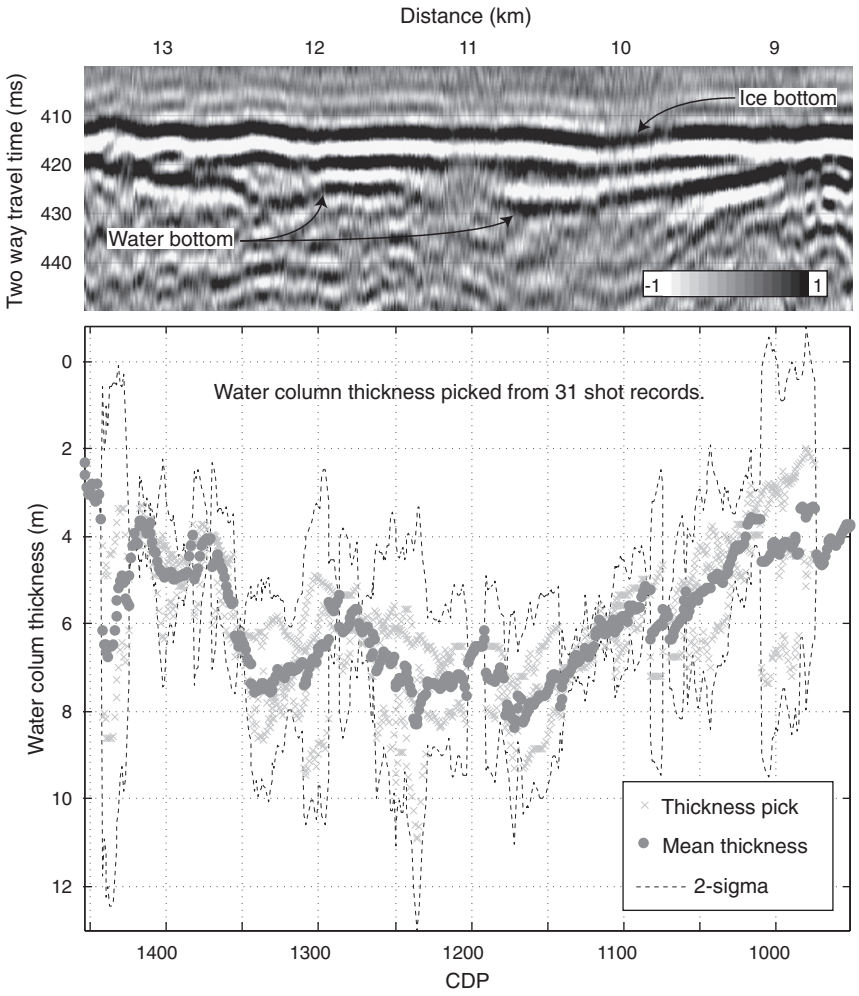

Fig. 7. Top: Longitudinal seismic profile zoom on imaged water column. Bottom: Thickness of the water column calculated from individual shot records.

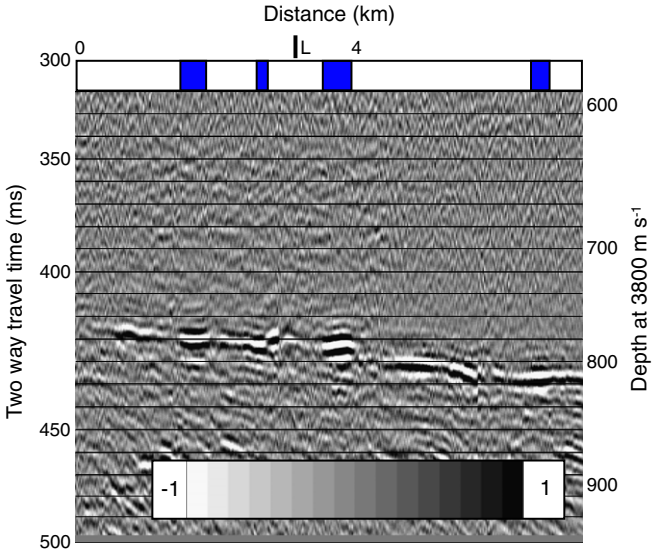

Fig. 8. Upstream transverse seismic profile. Ice stream flow is into the page. See Fig. 2 for location. The tick-mark annotated L denotes the intersection with the longitudinal line. Blue and white bar shows the zones of interpreted water (blue).

phase, as observed by Atre and Bentley (1993). Small-scale differences between our seismic picks and the remotely-sensed lake margins are not surprising considering the modulation of subglacial elevation changes by the overlying ice stream (Sergienko et al., 2007). However, the good correlation between the true-left (left of the flow direction) and true-right lake margins supports the active-lake perimeter picks of Fricker et al. (2007) and Fricker and Scambos (2009). At the downstream end of SLW the seismically resolved water extends 3.0 km beyond the active lake boundary, while at the upstream end, a significant portion of SLW appears to be free of seismically detectable water (kilometers 14.6–line end). The most upstream transverse profile indicates patchy water for the majority of the active lake width, which is supported by the late stage filling observed on ICESat track 0053 (Fig. 3). Downstream connectivity is indicated by the corresponding filling signal observed on ICESat track 0042. The middle and downstream transverse seismic-profiles show that water remains distributed but patchy for the full lateral extent of the active lake. The central portion of the longitudinal profile (kilometers 8.5–13.5) is the only section where the top and bottom of the water column are seismically imaged. This imaged water column is less than ~8 m thick (Fig. 7) and corresponds to the region of maximum ICESat range (Fig. 2) and the hydropotential low within the study area (Fig. 2, Christianson et al., 2012-this issue). The most suitable location for subglacial access is considered to be in the middle of this imaged water column at S 84.240° W 153.694°. Differences between the remotely sensed lake perimeter and that observed in the seismic data imply that SLW grounds or has

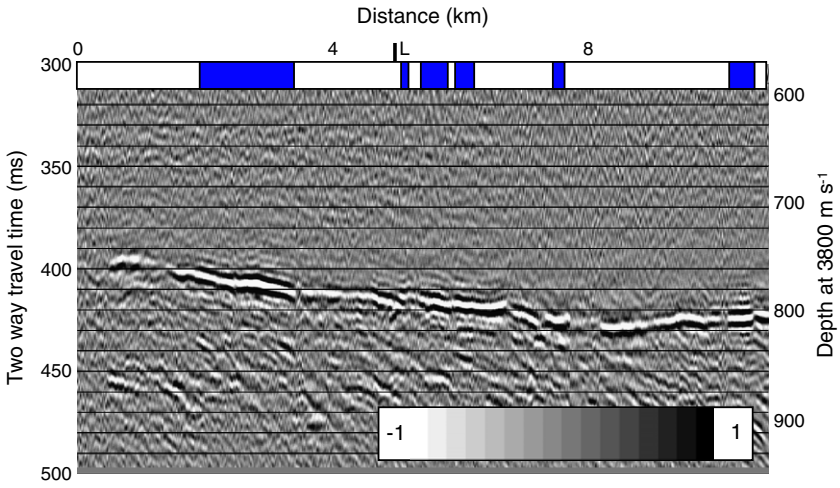

Fig. 9. Middle transverse seismic profile. Ice stream flow is into the page. See Fig. 2 for location. The tick-mark annotated L denotes the intersection with the longitudinal line. Blue and white bar shows the zones of interpreted water (blue).

negligible water in places at low-stands, or, has disconnected or transient active and inactive portions. It is also possible that SLW is a system in transition with sediment erosion and deposition changing the lake over time.

Active subglacial lakes affect the basal boundary of ice streams by concentrating the distribution of water in both space and time. In general the base of Whillans Ice Stream is accreting (Joughin et al., 2004) and the rapid motion of the ice stream is enabled by the efficient delivery of basal water from upstream (Parizek et al., 2003). Total basal melt for Whillans Ice Stream, including its catchment and tributaries, is estimated by Joughin et al. (2004) to be 0.53 $km^3\ a^{-1}$, which equates to an areal average production rate of 3.1 $mm\ a^{-1}$. This total consists of 0.16 $km^3\ a^{-1}$ (1.8 $mm\ a^{-1}$) from the catchment, 0.29 $km^3\ a^{-1}$ (7.7 $mm\ a^{-1}$) from the tributary region and only 0.07 $km^3\ a^{-1}$ (1.8 $mm\ a^{-1}$) from the ice stream itself. Beem et al. (2010) showed that for the majority of Whillans Ice Stream meltwater production is concentrated along the ice-stream margins. In light of the stick–slip motion of Whillans Ice Stream, Walter et al. (2011) estimated that during slip events Whillans is capable of generating basal meltwater, while in the intervening quiescent periods it is likely accreting. There are few additional constraints on the temporal variability of meltwater supply beneath Whillans Ice Stream, with the exception of Raymond (2000) who demonstrated that a decrease in the speed of Whillans Ice Stream, which is occurring (Joughin et al., 2005), should lead to an increase in meltwater production.

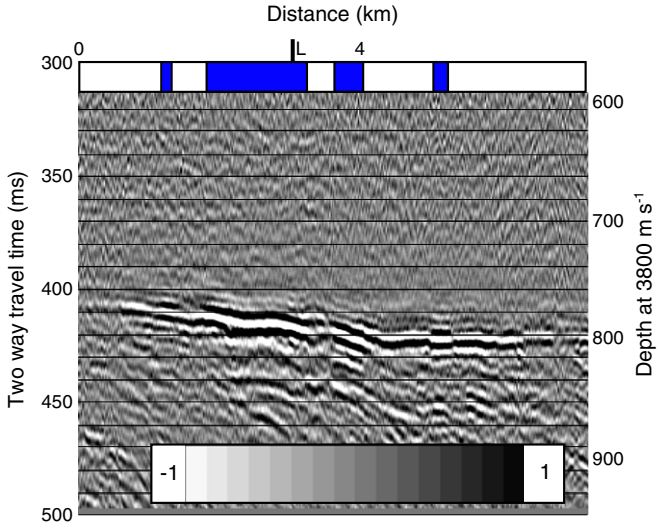

Fig. 10. Downstream transverse seismic profile. Ice stream flow is into the page. See Fig. 2 for location. The tick-mark annotated L denotes the intersection with the longitudinal line. Blue and white bar shows the zones of interpreted water (blue).

SLW is capable of retaining a significant proportion of the annual melt budget for Whillans Ice Stream. Smith et al. (2009) estimated volume changes for SLW, with a filling of 0.15 km^3 between March 2004 and June 2006. This filling indicates that SLW was receiving the equivalent of approximately 13% of the estimated annual meltwater production for Whillans Ice Stream during this period. This filling was followed by a decrease of 0.092 km^3 lasting until March 2007. Fricker et al. (2007) estimated a slightly lower filling volume of 0.13 km^3 followed by a 0.09 km^3 drainage. This drainage event was followed by a slight increase in lake volume of 0.023 km^3 before the final campaign reported by (Smith et al., 2009) in March 2008. Fig. 3 indicates that this filling was likely followed by a drainage event returning SLW to its previous low-stand state. Assuming adequate temporal sampling, this drainage event occurred at a lower water-pressure than the previous 2006–2007 drainage. Fricker and Scambos (2009) noted a correlation between lake size and location, and drainage duration, whereby the smaller subglacial lakes beneath the ice stream proper, such as SLW, drained faster than the larger lakes situated along the ice stream margin. Examining many more active lakes in Antarctica, Smith et al. (2009) related the drainage time of subglacial lakes to the hydropotential gradient, such that subglacial lakes in regions of low surface slope, such as SLW, are expected to drain more slowly than those in regions of high surface slope. Interestingly, the filling and drainage cycle of SLW (Fig. 3, Fricker & Scambos, 2009), while poorly sampled, does not indicate a sawtooth cycling of slow filling and rapid drainage as evident in subaerial jökulhlaups (e.g. Ng & Liu, 2009). We note that repeated small outburst floods such as those observed by (Winberry et al., 2009a) might appear as a smooth loss of lake volume if sampled at the resolution and accuracy of the available altimetry.

The most likely drainage system beneath a low-slope, soft-bedded ice stream such as Whillans Ice Stream, is a network of shallow canals incised in the underlying till (characteristic dimensions: ~0.1 m depth, and ~1 m width, spaced at 50–300 m, Engelhardt & Kamb, 1997; Walder & Fowler, 1994). During a rapid lake-drainage event, the downstream water-flux increase would likely result in an initial sheet flow, which would be unstable, and evolve into a system of

interfacial conduits, which in turn would evolve into a canal network (Walder & Fowler, 1994). It is noteworthy that such a canal network would be non-arborescent and below the resolution limits of our seismic methods. Any drainage mechanism needs to be consistent with the variable lake heights preceding the drainage events (Fig. 3) and the apparently symmetrical pattern of filling and drainage at SLW (Fricker & Scambos, 2009).

The longevity of subglacial lakes beneath active ice streams has significance for ice dynamics, subglacial biological communities, and subglacial limnology in general. Non steady-state behavior is well documented for the Siple coast ice streams (Retzlaff and Bentley, 1993; Hulbe and Fahnestock, 2007; Joughin et al., 2005); however, large reorganizations on Whillans Ice Stream are unlikely to have occurred during the last 460 years (Hulbe & Fahnestock, 2007). It is likely that SLW is considerably older than this, especially if the lake is bedrock-controlled as suggested by our seismic data. Subglacial sediment transport also makes it likely that SLW is currently diminishing in size. A longer term cycling of subglacial lakes may occur, whereby thicker and steeper ice in glacial times (Denton and Hughes, 2002) leads to less likelihood of surface slope reversals and lake formation, with a steeper hydropotential gradient driving water away; the resulting increase in bed coupling would favor erosion of sediments from a former lake, which in turn may be linked to lithologic or structural controls (e.g. Rooney et al., 1991). During interglacials the thinner ice and subsequent surface slope reversal would lead to lake formation. Sediment supply in the absence of erosion would lead to a gradual shallowing of the lake.

5. Summary and conclusions

SLW remains a shallow lake even in its low-stand state. The active lake extent as delineated by ICESat elevation range and image differencing (Fricker & Scambos, 2009; Fricker et al., 2007) compares well with seismic phase and amplitude observations. Seismic picks match the previous lake-edge estimates along the lateral margins but compare less well at the upstream and downstream ends of the lake. At the time of observation, the upstream end of the lake appeared to be free of water, but water appeared to be present at the downstream end, although the thickness of water was less than could be resolved by our seismic measurements. Between these, a shallow water column is imaged along the center of the lake, with thicknesses estimated to be 3–8 m. Maximum ICESat elevation range and a hydropotential low calculated from surface GPS and radar data (Christianson et al., 2012-this issue) support the interpretation of a water column at this location. The upstream and downstream ends of the water column correspond with acoustic basement features. The imaged water column is considered the most suitable location for subglacial exploration of this active lake.

Supplementary materials related to this article can be found online at doi:10.1016/j.epsl.2012.02.023.

Acknowledgments

This experiment was carried out as part of the WISSARD program funded by the American Recovery and Reinvestment Act of 2009 through the National Science Foundation (NSF OPP 0838763, 0838855). We thank Slawek Tulaczyk and Helen Fricker for their involvement in field planning. We are grateful to Ben Smith for advice on ICESat data processing, and to Ian Joughin for providing velocity data. Mauro Pavan is thanked for his invaluable assistance in the field. NSIDC is thanked for their distribution of ICESat and MODIS MOA data. HJH acknowledges the generous support of the Alan Eggers Endowment. This manuscript was improved by the comments of two anonymous reviewers and discussions with Ružica Dadić.

References

Anandakrishnan, S., 2003. Dilatant till layer near the onset of streaming flow of Ice Stream C, determined by AVO (Amplitude vs. Offset) analysis. Ann. Glaciol. 36, 283–287.
Atre, S.R., Bentley, C.R., 1993. Laterally varying basal conditions under Ice Streams B and C, West Antarctica. J. Glaciol. 39, 507–514.
Beem, L.H., Jezek, K.C., Van der Veen, C.J., 2010. Basal melt rates beneath Whillans Ice Stream, West Antarctica. J. Glaciol. 56 (198), 647–654.
Bell, R.E., Studinger, M., Shuman, C.A., Fahnestock, M.A., Joughin, I., 2007. Large subglacial lakes in East Antarctia at the onset of fast-flowing ice streams. Nature 445, 904–907.
Bell, R.E., Ferraccioli, F., Creyts, T.T., Braaten, D., Corr, H.F.J., Das, I., Demaske, D., Frearson, N., Jordan, T., Rose, K., Studinger, M., Wolovick, M., 2011. Widespread persistent thickening of the East Antarctic Ice Sheet by freezing from the base. Science 331, 1592–1595.
Bindschadler, R.A., King, M.A., Alley, R.B., Anandakrishnan, S., Padman, L., 2003. Tidally controlled stick–slip discharge of a West Antarctic ice stream. Science 301, 1087–1089.
Carcione, J.E.M., Gei, D., 2003. Seismic modelling study of a subglacial lake. Geophys. Prospect. 51 (6), 501–515.
Carter, S., Blankenship, D.D., Peters, M.E., Young, D.A., Holt, J.W., Morse, D.L., 2007. Radar-based subglacial lake classification in Antarctica. Geochem. Geophys. Geosyst. 8 (3), 1–20.
Christianson, K., Jacobel, R.W., Horgan, H.J., Anandakrishnan, S., Alley, R.B., 2012. Subglacial Lake Whillans — Ice-penetrating radar and GPS observations of a shallow active reservoir beneath a West Antarctic ice stream. Earth and Planetary Science Letters. 331–332, 237–245 (this issue).
Denton, G.H., Hughes, T.J., 2002. Reconstructing the Antarctic ice sheet at the last glacial maximum. Quat. Sci. Rev. 21, 193–202.
Engelhardt, H., Kamb, W.B., 1997. Basal hydraulic system of a West Antarctic ice stream: constraints from borehole observations. J. Glaciol. 43 (144), 207–230.
Engelhardt, H., Humphrey, N., Kamb, W.B., Fahnestock, M., 1990. Physical conditions at the base of a fast moving Antarctic ice stream. Science 248, 57–59 Apr.
Fowler, C.M.R., 1990. The Solid Earth: An Introduction to Global Geophysics, 1st Edition. Cambridge University Press.
Fricker, H.A., Scambos, T., 2009. Connected subglacial lake activity on lower Mercer and Whillans Ice Streams, West Antarctica, 2003–2008. J. Glaciol. 55 (190), 303–315.
Fricker, H.A., Scambos, T.A., Bindschadler, R.A., Padman, L., 2007. An active subglacial water system in West Antarctica mapped from space. Science 315 (1544), 1544–1548.
Fricker, H.A., Powell, R.D., Priscu, J.C., Tulaczyk, S., Anandakrishnan, S., Christner, B., Fisher, A.T., Holland, D.M., Horgan, H.J., Jacobel, R.W., Mikucki, J., Mitchell, A., Scherer, R., Severinghaus, J.P., 2011. Siple Coast subglacial aquatic environments: the Whillans Ice Stream Subglacial Access Research Drilling (WISSARD) project. AGU Monograph. American Geophysical Union. Ch. 12.
Gray, L., Joughin, I., Tulaczyk, S., Spikes, V.B., Bindschadler, R.A., Jezek, K.C., 2005. Evidence for subglacial water transport in the West Antarctic Ice Sheet through three-dimensional satellite radar interferometry. Geophys. Res. Lett. 32 (L03501).
Haran, T., Bohlander, J., Scambos, T., Fahnestock, M., 2005. MODIS mosaic of Antarctica (MOA) image map. NSIDC Digital media.
Hulbe, C.L., Fahnestock, M.A., 2007. Century-scale discharge stagnation and reactivation of the Ross Ice Streams, West Antarctica. J. Geophys. Res. 112 (F03S27).
Iken, A., Bindschadler, R.A., 1986. Combined measurements of subglacial water pressure and surface velocity of Findelengletscher, Switzerland: conclusions about drainage system and sliding mechanism. J. Glaciol. 32 (110), 101–119.
Joughin, I., pers comm 2008. Antarctic velocity mosaic from combined interferometric and speckle tracking techniques. personal communication.
Joughin, I., Tulaczyk, S., Bindschadler, R.A., Price, S.F., 2002. Changes in West Antarctic ice stream velocities: observation and analysis. J. Geophys. Res. 107 (B11). doi:10.1029/2001JB001029.
Joughin, I., Tulaczyk, S., MacAyeal, D.R., Engelhardt, H.F., 2004. Melting freezing beneath the Ross ice streams, Antarctica. J. Glaciol. 50 (168), 96–108.
Joughin, I., Bindschadler, R.A., King, M.A., Voigt, D.E., Alley, R.B., Anandakrishnan, S., Horgan, H.J., Peters, L.E., Winberry, P., Das, S.B., Catania, G.A., 2005. Continued deceleration of Whillans Ice Stream, West Antarctica. Geophys. Res. Lett. 32. doi:10.1029/2005GL024319.
Kamb, B., 2001. Basal zone of the West Antarctic ice streams and its role in the lubrication of their rapid motion. of In: Alley, R.B., Bindschadler, R.A. (Eds.), The West Antarctic Ice Sheet: Behavior and Environment. : Antarctic Research Series, Vol. 77. AGU, pp. 157–200.
Kapitsa, A.P., Ridley, J.K., Robin, G.d.Q., Siegert, M.J., Zotikov, I.A., 1996. A large deep freshwater lake beneath the ice of central East Antarctica. Nature 381, 684–686.
King, E.C., Woodward, J., Smith, A.M., 2004. Seismic evidence for a water-filled canal in deforming till beneath Rutford Ice Stream, West Antarctica. Geophys. Res. Lett. 31 (L20401), 1–4.
Ng, F., Liu, S., 2009. Temporal dynamics of a jökulhlaup system. J. Glaciol. 55 (192), 651–665.
Parizek, B.R., Alley, R.B., Hulbe, C.L., 2003. Subglacial thermal balance permits ongoing grounding-line retreat along the Siple Coast of West Antarctica. Ann. Glaciol. 36, 251–256.
Peters, L.E., Anandakrishnan, S., Alley, R.B., Smith, E., 2007. Extensive storage of basal meltwater in the onset region of a major West Antarctic ice stream. Geology 35 (3), 251–254.
Peters, L.E., Anandakrishnan, S., Holland, C.W., Horgan, H.J., Blankenship, D.D., Voigt, D.E., 2008. Seismic detection of a subglacial lake near the South Pole, Antarctica. Geophys. Res. Lett. 35 (L23501), 1–5.
Pritchard, H.D., Arthern, R.J., Vaughan, D.G., Edwards, L.A., 2009. Extensive dynamic thinning on the margins of the Greenland and Antarctic ice sheets. Nature 461, 971–975.

Raymond, C.F., 2000. Energy balance of ice streams. J. Glaciol. 46 (155), 665–674.
Retzlaff, R., Bentley, C.R., 1993. Timing of stagnation of Ice Stream C, West Antarctica from short-pulse-radar studies of buried surface crevasses. J. Glaciol. 39, 553–561.
Rooney, S.T., Blankenship, D.D., Alley, R.B., Bentley, C.R., 1991. Seismic reflection profiling of a sediment-filled graben beneath Ice Stream B, West Antarctica. In: Thomson, M.R.A., Crame, J.A., Thomson, J.W. (Eds.), Geological Evolution of Antarctica. Cambridge University Press, Cambridge, pp. 261–265.
Rose, K.E., 1979. Characteristics of ice flow in Marie Byrd Land, Antarctica. J. Glaciol. 24 (90), 63–74.
Röthlisberger, H., 1972. Water pressure in intra- and subglacial channels. J. Glaciol. 11 (62), 177–203.
Schoof, C., 2010. Ice-sheet acceleration driven by melt supply variability. Nature 468, 803–806.
Sergienko, O.V., MacAyeal, D.R., Bindschadler, R.A., 2007. Causes of sudden, short-term changes in ice-stream surface elevation. Geophys. Res. Lett. 34 (L22503), 1–6.
Siegert, M.J., Hindmarsh, R., Corr, H., Smith, A., Woodward, J., King, E.C., Payne, A.J., Joughin, I., 2004. Subglacial Lake Ellsworth: a candidate for in situ exploration in West Antarctica. Geophys. Res. Lett. 31, L23403. doi:10.1029/2004GL021477.
Siegert, M.J., Carter, S., Tabacco, I., Popov, S., Blankenship, D.D., 2005. A revised inventory of Antarctic subglacial lakes. Ant. Sci. 17 (3), 453–460.
Smith, B.E., Bentley, C.R., Raymond, C.F., 2005. Recent elevation changes on the ice streams and ridges of the Ross Embayment from ICESat crossovers. Geophys. Res. Lett. 32 (L21S09), 1–5.
Smith, B.E., Fricker, H.A., Joughin, I.R., Tulaczyk, S., 2009. An inventory of active subglacial lakes in Antarctica detected by ICESat (2003–2008) tarctica detected by icesat (2003–2008). J. Glaciol. 55 (192), 573–593.
Stearns, L.A., Smith, B.E., Hamilton, G.S., 2008. Increased flow speed on a large East Antarctic outlet glacier caused by subglacial floods. Nat. Geosci. 1, 827–831.
Studinger, M., Bell, R.E., Karner, G.D., Tikku, A.A., Holt, J.W., Morse, D.L., Richter, T.G., Kempf, S.D., Peters, M.E., Blankenship, D.D., Sweeney, R.E., Rystrom, V.L., 2003. Ice cover, landscape setting, and geological framework of Lake Vostok, East Antarctica. Earth Planet. Sci. Lett. 205 (3–4), 195–210.
Thigpen, B.B., Dalby, A.E., Landrum, R., 1975. Special report of the subcommittee on polarity standards. Geophysics 40, 694–699.
Vaughan, D.G., Rivera, A., Woodward, J., Corr, H.F.J., Wendt, J., Zamora, R., 2007. Topographic and hydrological controls on Subglacial Lake Ellsworth, West Antarctica. Geophys. Res. Lett. 34 (L18501), 1–5.
Walder, J.S., Fowler, A.C., 1994. Channelised subglacial drainage over a deformable bed. J. Glaciol. 40, 3–15.
Walter, J.I., Brodsky, E.E., Tulaczyk, S., Schwartz, S.Y., Pettersson, R., 2011. Transient slip events from near-field seismic and geodetic data on a glacier fault, Whillans Ice Plain, West Antarctica. J. Geophys. Res. 116 (F01021).
Winberry, J.P., Anandakrishnan, S., Alley, R.B., 2009a. Seismic observations of transient subglacial water-flow beneath MacAyeal Ice Stream, West Antarctica. Geophys. Res. Lett. 36 (L11502), 1–5.
Winberry, J.P., Anandakrishnan, S., Alley, R.B., Bindschadler, R.A., King, M.A., 2009b. Basal mechanics of ice streams: insights from the stick–slip motion of Whillans Ice Stream, West Antarctica. J. Geophys. Res. 114 (F01016), 1–11.
Wingham, D.J., Siegert, M.J., Shephard, A., Muir, A.S., 2006. Rapid discharge connects Antarctic subglacial lakes. Nature 440, 1033–1036 April.
Woodward, J., Smith, A.M., Ross, N., Thoma, M., Corr, H.F.J., King, E.C., King, M.A., Grosfeld, K., Tranter, M., Siegert, M.J., 2010. Location for direct access to Subglacial Lake Ellsworth: an assessment of geophysical data and modeling. Geophys. Res. Lett. 37, L11501 Jun.
Zwally, H.J., Abdalai, W., Herring, T., Larson, K., Saba, J., Steffen, K., 2002. Surface melt-induced acceleration of Greenland Ice-Sheet flow. Science 297 (5579), 218–221.